NUMERICAL STUDY OF CRACKED TRISO PARTICLES WITH RANDOM SIZE AND LOCATION DISTRIBUTIONS IN FCM FUEL ELEMENTS: EFFECTS ON TEMPERATURE DISTRIBUTION

CHUNXI WU[1], WEI ZHANG[1], GUITAO YANG[1], TENGLONG CONG[1]
School of Nuclear Science and Engineering, Shanghai Jiao Tong University
200240 Shanghai, P.R. China

MAOLONG LIU[2*]
Institute of Modern Physics, Fudan University
200433 Shanghai, P.R. China

ABSTRACT

During reactor operation, the exact size values or specific size distribution of tri-structural isotropic (TRISO) fuel particles randomly dispersed within the fully ceramic microencapsulated (FCM) fuel elements are often unknown. Additionally, as burnup increases, elastic, thermal, and irradiation-induced strains between different layers of TRISO fuel particles may lead to the formation of cracks, introducing additional thermal resistance between the layers and affecting the accurate prediction of temperature. To investigate the impact of the additional thermal resistance caused by cracks in TRISO particles with random size and position distributions, TRISO fuel particles with diameter randomized from a Gaussian distribution and position randomly distributed in the FCM fuel element are generated using relevant algorithms. A certain proportion of TRISO fuel particles are randomly selected to acquire additional thermal resistance between layers. Through numerical simulation, a three-dimensional temperature field distribution of the fuel element is obtained. The conclusions of this study provide reference information for predicting the temperature distribution of FCM fuel elements containing TRISO particles with random size and location distributions, taking into account the presence of cracks.
Keywords: TRISO fuel particles, Numerical simulation, Random distribution, Crack

1. Introduction

1.1. Background

Fully Ceramic Microencapsulated (FCM) fuel is a type of accident-tolerant fuel composed of TRi-structural ISOtropic (TRISO) fuel particles embedded in a ceramic matrix. Hence, it is also referred to as TRISO-based FCM fuel. The matrix material can be silicon carbide or other ceramic materials with excellent mechanical, thermal conductivity, and radiation resistance properties. Typical TRISO particles consist of a four-layer encapsulation structure, comprising a pyrolytic carbon (buffer) layer, an inner pyrolytic carbon (IPyC) layer, a silicon carbide (SiC) layer, and an outer pyrolytic carbon (OPyC) layer successively coated over a fuel kernel. The buffer layer primarily accommodates fission products, reducing radiation damage to other layers, and kernel swelling. The IPyC layer serves to protect the SiC layer from fission products. The SiC layer primarily serves as the main fission product retention barrier, while the OPyC layer shields the SiC layer from damage [1]. Currently, various reactor types, such as High-temperature Gas-cooled Reactors (HTGRs), Fluoride-salt-cooled High-temperature Reactors (FHRs), and Very High-temperature Reactors (VHTRs), are utilizing TRISO-based FCM fuel to withstand harsh operating conditions, thereby improving safety [2].

Due to the unique manufacturing process of TRISO-based FCM fuel, the position of TRISO

particles within the matrix is random. Moreover, as burnup increases, the inner dimensions of TRISO particles can change. Additionally, cracks may occur within the particles due to the effects of elastic, thermal, and irradiation-induced stresses between different layers. This can introduce additional thermal resistance, reducing the effective thermal conductivity of TRISO particles and thereby affecting fuel performance. Therefore, this study aims to investigate the impact of reduced particle thermal conductivity caused by cracks on the temperature distribution in FCM fuel containing randomly dispersed particles varying in size. Furthermore, sensitivity analysis is conducted on the contribution of the proportion of cracked particles and the additional porosity brought by cracks to the temperature distribution of the FCM pellet.

1.2. Previous studies

The generation of cracks in TRISO particles is a critical form of fuel failure. To date, several scholars have conducted research on the mechanisms of crack generation, crack morphology under various conditions, and their effects. Wang [3], combining experimental and fracture mechanics theory methods, analyzed the mechanisms of crack generation and propagation in the IPyC, OPyC, and SiC layers of TRISO particles and established a PyC crack-induced fuel failure model. This study suggests that tangential stresses continuously increase due to factors such as fission gas accumulation, leading to radial cracking of the IPyC layer. The cracks propagate continuously towards the boundary of the SiC layer. Due to factors such as creep crack extension and fatigue loading, a crack may breach the harder SiC layer boundary, continuing to propagate to the OPyC layer, thereby leading to fuel failure. Idaho National Laboratory [4] developed a model called PARFUME (Particle Fuel Model) for analyzing the performance of TRISO fuel particles. This model considers fuel failure caused by shrinkage cracks in the IPyC layer and has subsequently been applied to studies on TRISO fuel particle failure probability and design optimization [5]. Haynes et al. [6] established a two-dimensional peridynamic model of TRISO particles using the finite element method and analyzed crack morphology in each layer of TRISO particles under normal operation (nuclear power of 0.267 W per particle) and extreme accident conditions (1.60 W per particle. The study found that cracks originate from the fuel kernel and gradually extend outward. Under normal conditions, a crack cannot penetrate the buffer layer until extreme conditions exceed 940% of nuclear power (2.51 W per particle), where the crack can penetrate the silicon carbide layer, leading to the release of fission gas.

The aforementioned studies mainly focus on fuel failure caused by cracks and mostly investigate single TRISO particles. However, there is scarce mention of the impact on the thermal conductivity of TRISO particles of additional thermal resistance caused by cracks, which in turn affects the temperature distribution in TRISO-based FCM fuel. Regarding FCM fuel with randomly dispersed TRISO particles in the matrix, various models for equivalent thermal conductivity or temperature distribution have been developed, as shown in the table below. By determining the equivalent thermal conductivity of TRISO particles and matrix composite materials, the temperature field can be approximated and predicted based on a homogeneous assumption. However, apart from the two-regime model, the following models have not taken into account the impact of the random distribution of TRISO particle sizes, which imposes certain limitations.

Model name	Correlation
Maxwell[7]	$\frac{k_e}{k_m} = \frac{1+2\beta\phi}{1-\beta\phi}$
Reduced Maxwell[7]	$\frac{k_e}{k_m} = \frac{1+\beta\phi}{1-0.5\beta\phi}$
Chiew and Glandt [8]	$\frac{k_e}{k_m} = \frac{1+2\beta\phi+(2\beta^3-0.1\beta)\phi^2+0.05\phi^3 e^{4.5\beta}}{1-\beta\phi}$
Bruggeman [9]	$\frac{k_e}{k_m} = \kappa A + (\kappa^2 A^2 + 0.5\kappa)^{0.5}, A = 0.25(3\phi - 1 + \frac{2-3\phi}{\kappa})$

Two-regime[10,11]	$T = \begin{cases} \frac{q_1''' R_1^2}{2k_m} ln\left(\frac{R_p}{R_1}\right) + \frac{q_1'''}{4k_1}(R_1^2 - r^2) + T_R \text{ , } 0 \le r \le R_1 \\ \frac{q_1''' R_1^2}{2k_m} ln\left(\frac{R_p}{r}\right) + T_R \text{ , } R_1 \le r \le R_p \end{cases}$ $R_1 = \sqrt{\frac{\phi}{\phi_{max}}} R_p \text{ , } for\ cylinder\ matrix$

Tab. 1 Thermal conductivity or temperature distribution models

Where ϕ is packing fraction, β and κ are defined by Equation (1).

$$\beta = \frac{\kappa - 1}{\kappa + 2} \text{ , } \kappa = \frac{k_p}{k_m} \quad (1)$$

Due to the manufacturing process of numerous TRISO particles, the size of TRISO fuel particles is not constant but follows random distribution patterns, including a Gaussian distribution. Hence, in this study, TRISO particles randomly dispersed in the matrix with sizes following a Gaussian distribution are generated using relevant algorithms to account for the particle-to-particle statistical variations in fuel properties that arise from the TRISO fuel fabrication process. Meanwhile, a certain proportion of TRISO particles is selected randomly to appropriately reduce the thermal conductivity, which means a random fraction of TRISO particles is assigned a lower thermal conductivity to simulate cracks in their coating layers. This process is further described in section 2.2. Finally, the temperature field distribution of the FCM fuel element is obtained through numerical simulation.

2. Numerical simulation

2.1. Random generation of TRISO particles

This study utilizes the "neighbor-based generation algorithm" to generate TRISO particles within the FCM fuel matrix. The algorithm randomly selects an already-generated particle and utilizes the Marsaglia method [12] to search for a non-overlapping region on a spherical surface concentric with the selected particle and a radius equal to the sum of the radius of the selected particle and the particle to be generated. If no such region is found, another already-generated particle is selected, and the process is repeated until a suitable position for filling is found. This method enhances the efficiency of particle generation under high packing fractions while maintaining a certain level of randomness. This, in turn, reduces the time required for random generation to an acceptable range. The specific process of obtaining the central coordinates of the required fuel particles using this algorithm is illustrated in Fig. 1. Moreover, for the generation of randomly distributed particle diameters, considering the required diameters d_g to follow a Gaussian distribution within [d-Δd, d+Δd], based on the principles of rare events and hypothesis testing, it can be assumed that $d_g \sim N(d, (\Delta d)^2/9)$. In this study, the mean value of particle diameter d is 0.33 mm and Δd is 0.04 mm.

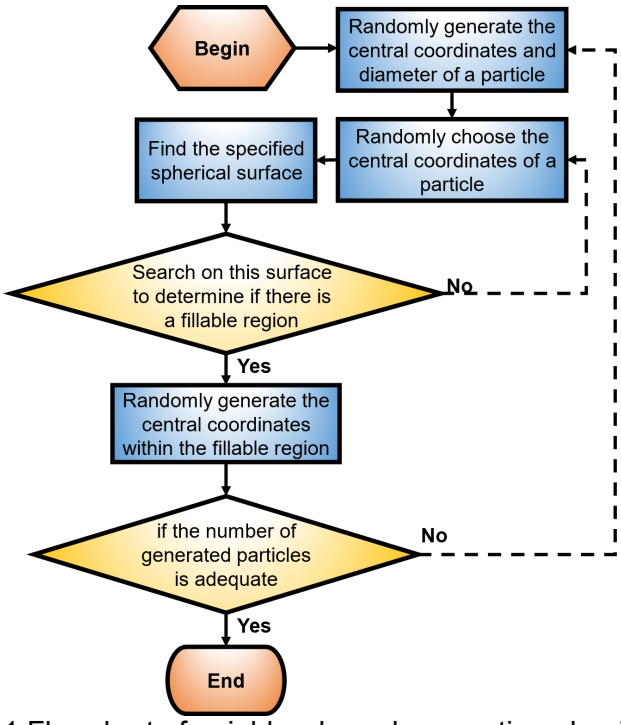

Fig. 1 Flowchart of neighbor-based generation algorithm

2.2. Additional thermal resistance caused by crack

In this study, the proportion of cracked particles *f* and the additional porosity *P* caused by cracks are selected as the parameters of interest for sensitivity analysis. Based on the summary from reference [6], the porosity correction of the equivalent thermal conductivity of TRISO particles can be expressed by Equation (2). After generating TRISO particles with random size and position distribution, a specific proportion of particles, corresponding to the proportion *f* of cracked particles, is randomly selected from the total number of particles. Then, based on the following Equation (2), the equivalent thermal conductivity of these particles is corrected according to the additional porosity *P*.

$$k = k_0 \frac{1-P}{1+(\sigma_S-1)P} \tag{2}$$

where k_0 and k are the equivalent thermal conductivity of TRISO particles before and after correction, respectively, P is the additional porosity, and σ_s is a shape factor, set equal to 1.5 for spherical shapes.

2.3. Numerical model

ANSYS software is used for geometric modeling and numerical simulation. The simulation utilized the geometry parameters for the cylindrical matrix and particles outlined in references [10,11,13]. Also, considering the complexity of modeling, appropriate simplification of homogeneous particles is applied to the multi-layer structure of TRISO fuel. Graphite is used for modeling the matrix material. The parameters for the simulated matrix and particle sizes are listed in the table below.

Cylinder radius (mm)	Cylinder height (mm)	Matrix thermal conductivity [W/(m·K)]	TRISO particle equivalent thermal conductivity (no crack) [W/(m·K)]	Particle radius (mm)	Packing fraction
3.9	3.9	25	3.77	0.29 ~0.37	0.3

Tab. 2 Parameters of the numerical model

After conducting mesh sensitivity analysis, a grid size of 0.1 mm is selected for generating unstructured grids. Ideal adiabatic boundary conditions are applied to the top and

bottom surfaces of the cylindrical matrix, while isothermal boundary conditions are applied to the side surface with a boundary temperature at T_{out} = 800 °C. Additionally, internal heat source boundary conditions are applied to all fuel particles with parameters set to q''' = 10^9 W/m^3. This value is used as the heat generation rate of TRISO particles for all cases in this study and is calculated by equation (3), where the linear power and packing fraction are 200 W/cm and 0.42 [14], respectively. A schematic diagram of the boundary conditions is shown in Fig. 2.

$$q''' = \frac{q'H}{\phi V_{matrix}} \tag{3}$$

Where q' is the linear power, H is the height of cylindrical matrix, ϕ is the packing fraction and V_{matrix} is the volume of cylindrical matrix.

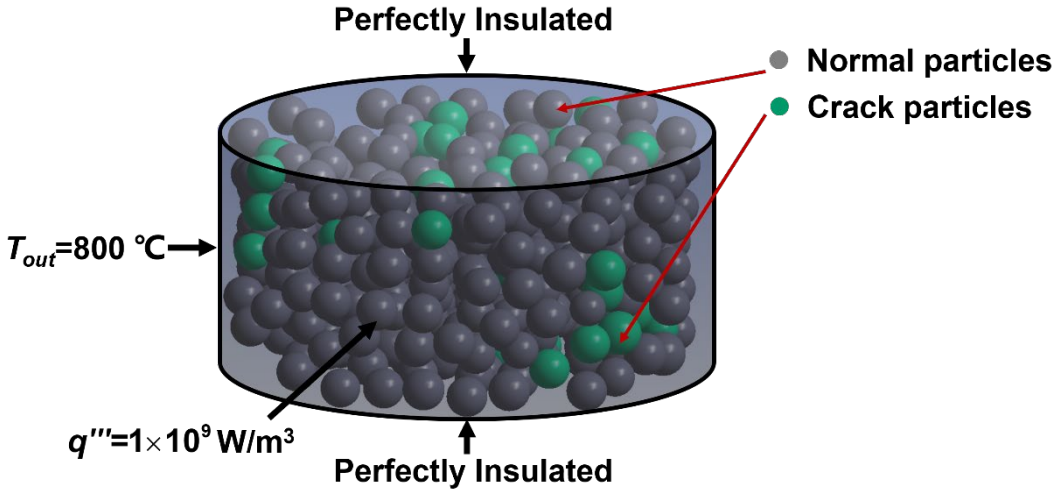

Fig. 2 Boundary condition

2.4. Simulation cases

The study randomly generates 60 different scenarios within a cylindrical matrix at a packing fraction of 30%, resulting in 60 baseline sub-cases. Each sub-case corresponds to a random distribution in size and location of TRISO particles and involves reductions in the equivalent thermal conductivity of some random particles with varying proportions of cracked particles and additional porosity caused by cracks. Although the overall porosity of TRISO particles are ~20%, the range of additional porosity caused by cracks is set to 0~50% in order to consider the extreme scenarios. This leads to the formation of 21 sets of cases, with each set comprising 60 baseline sub-cases. In the simulation analyzed below, the thermal conductivity changes radially based on the presence or absence of an intact or cracked TRISO particle. The specific parameters for each set are provided in the table below.

Case Set number	Proportion of cracked particles *f*	Additional porosity *P*	TRISO particle equivalent thermal conductivity [W/(m·K)]
1	0	0	3.770
2	10%	5%	3.494
3	20%	2%	3.658
4	20%	5%	3.494
5	20%	10%	3.231
6	30%	5%	3.494
7	50%	5%	3.494
8	50%	10%	3.231
9	50%	15%	2.981
10	50%	30%	2.295
11	50%	50%	1.508

12	70%	5%	3.494
13	70%	10%	3.231
14	70%	15%	2.981
15	70%	30%	2.295
16	70%	50%	1.508
17	100%	5%	3.494
18	100%	10%	3.231
19	100%	15%	2.981
20	100%	30%	2.295
21	100%	50%	1.508

Tab. 3 Simulation cases

2.5. Model validation

The study compares the results of radial temperature field calculations at the central cross-section of the matrix for 60 sub-scenarios without cracks with various heat conduction models introduced in Section 1.2, as shown in Fig. 3. The effective thermal conductivity values obtained by Maxwell, Bruggerman and Chiew & Glandt model are 17.057 W/(m·K), 16.430 W/(m·K) and 16.894 W/(m·K), respectively. The purple area in Fig. 3 represents the region enclosed by the upper and lower envelope lines of the axial temperature fields at the central cross-section of 60 sub-scenarios. For example, Fig. 4 illustrates how this area is determined. From Fig. 3, it can be observed that the simulation results are in good agreement with the calculations from the relevant models, indicating that the established numerical model is sufficiently reliable.

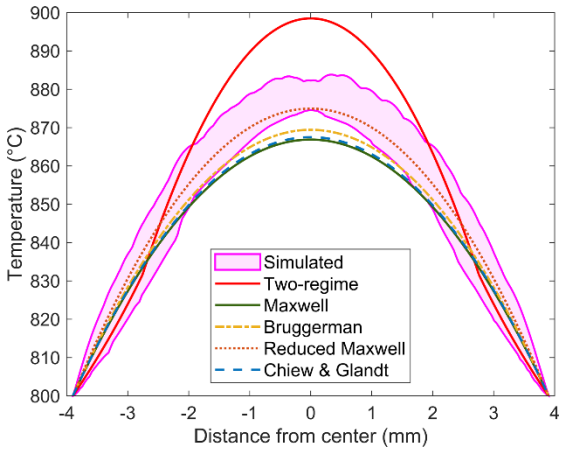

Fig. 3 Model validation

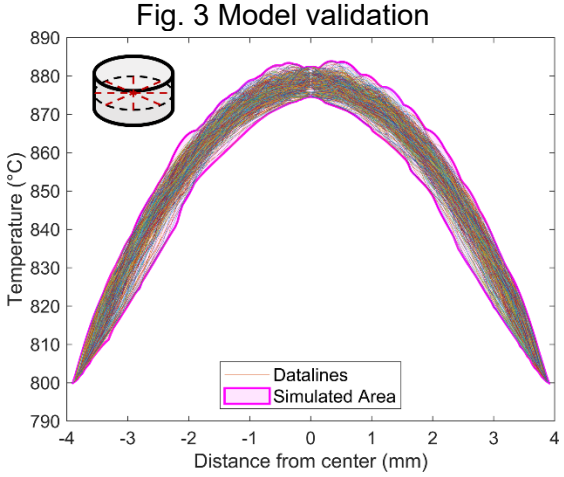

Fig. 4 Schematic diagram of the shaded area

3. Results

3.1. Overall temperature distribution

Fig. 5 illustrates the temperature distribution contours of particles and matrix under a scenario with the same geometry for Case Set 1 (no crack) and the most extreme Case Set 21 (f=100%, P=50%). It can be observed from Fig. 5 that, under both scenarios with and without cracks, the temperature of the FCM fuel decreases radially outward from the center, forming a hot zone in the central region. However, from the matrix cross-sectional view, it is evident that the temperature distribution in the central hot zone is more discrete when cracks are present in the particles, leading to localized hot spots with higher peak temperatures.

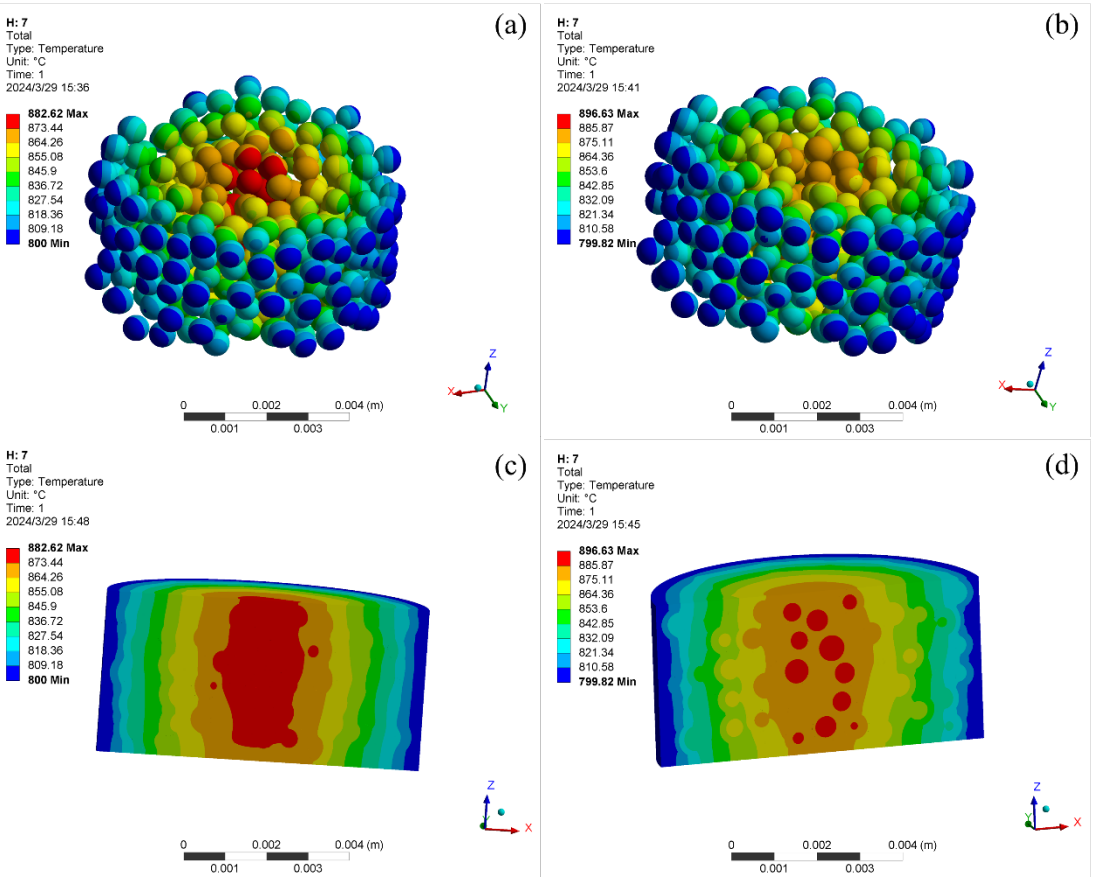

Fig. 5 Overall temperature contour: (a) Case Set 1, particles; (b) Case Set 21, particles; (c) Case Set 1, matrix; (d) Case Set 21, matrix

3.2. Maximum temperature

Fig. 6 illustrates the variation of the mean and standard deviation of the distributions of maximum temperature for 60 sub-scenarios in each case set varying the proportions of cracked particles f and the additional porosity P caused by cracks. Each data point in Fig. 6 corresponds to the result of a Case Set where only lines with more than one data point are listed based on the same P or f. Except for Case Set 1 (P=f=0), other single data points are hidden, such as Case Set 3 in Fig. 6a and b, and Case Set 2 and 6 in Fig. 6c and d.

From the perspective of the mean maximum temperature, there is a positive correlation with both the proportions of cracked particles and the additional porosity caused by cracks, but their changing patterns differ. Fig. 6a illustrates a linear relationship between the mean value of the maximum temperature and the proportions of cracked particles at a certain level of additional porosity, with relatively small overall variations. However, as the additional porosity increases, the variation amplitude also increases. Conversely, Fig. 6c shows an approximately exponential relationship between the mean maximum temperature and the additional porosity, with a tendency towards linearity as the proportions of cracked particles increase. Overall, the variation in the mean maximum temperature is more pronounced with

changes in the additional porosity, but the magnitude of variation with both factors is small. A peak temperature increase of approximately 0.9% or higher (ΔT_{max} > 8 °C) may occur in case sets with an additional porosity of 50%, reaching a maximum of approximately 1.4% (ΔT_{max} = 12.2 °C) for 100% cracked particles.

In terms of the standard deviation, it is positively correlated with the additional porosity. It initially increases and then decreases with an increase in the proportions of cracked particles. On one hand, this occurs because the positions and sizes of cracked particles are randomly distributed, which contributes to an increase in the standard deviation as the proportion increases. On the other hand, as more cracked particles appear, the randomness introduced by the random positions and sizes of uncracked particles decreases, leading to a negative impact on the standard deviation. The combined effects of these two factors result in a peak standard deviation occurring around 50% of cracked particles.

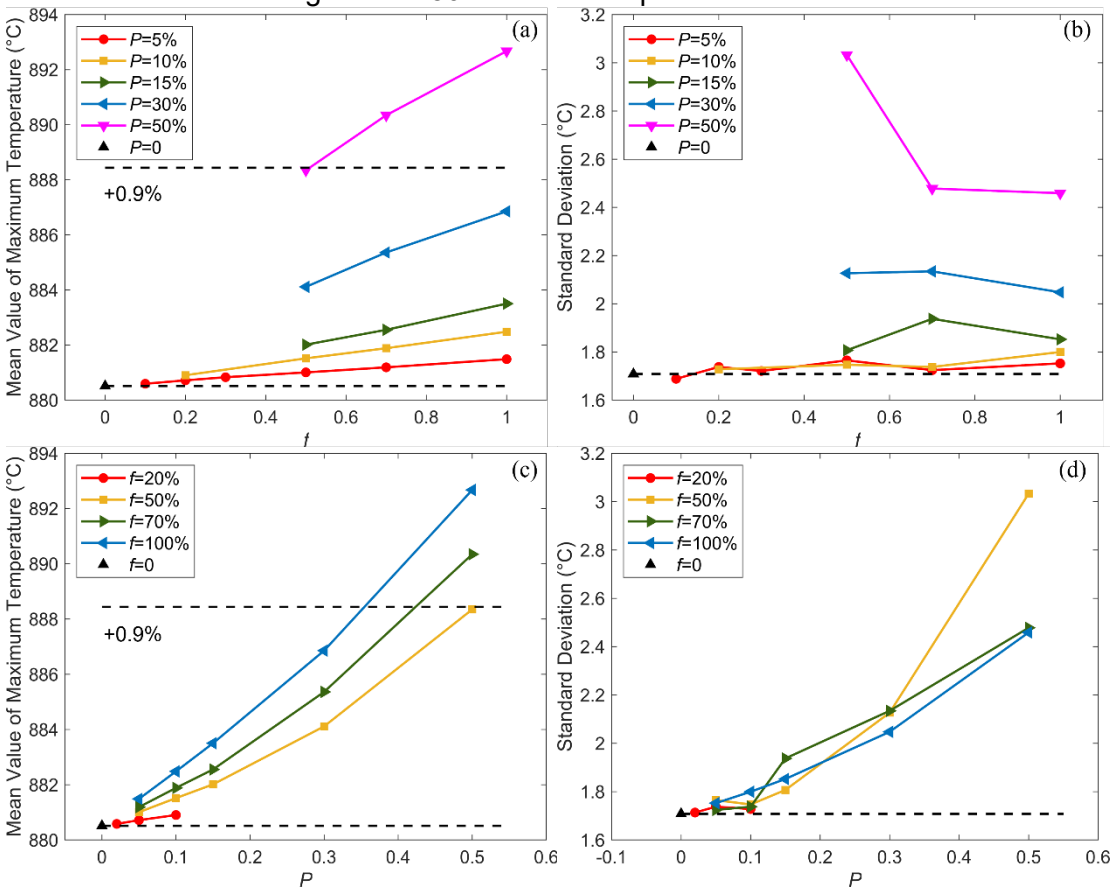

Fig. 6 Maximum temperature: (a) Mean value vs. proportion of cracked particles *f*; (b) Standard deviation vs. proportion of cracked particles *f*; (c) Mean value vs. additional porosity *P*; (d) Standard deviation vs. additional porosity *P*

3.3. Radial temperature distribution

Due to the symmetry of the cylindrical matrix, the following analysis focuses on the radial temperature distribution at the central cross-section of the matrix. Fig. 7 compares the radial temperature distributions of four typical case sets with the case set without crack and the results of typical models. The shaded areas in Fig. 7 represent the regions enclosed by the upper and lower envelope lines of the temperature distributions for 60 sub-scenarios in each case set.

Fig. 7a indicates that the radial temperature distribution is almost identical to that without a crack under conditions where the crack is less prevalent (cracked particle proportion < 50%, additional porosity < 10%). In general, from (a) to (d), the increase in porosity has a more significant effect on the radial temperature distribution than the proportion of cracked particles. The combined effect of these two factors broadens the potential range of radial temperature distribution band.

Furthermore, regardless of the presence of cracks, the radial temperature distribution at the central cross-section of the matrix within the central hot zone falls between the results calculated by the two-regime and Maxwell models. Even under the most extreme case set (f=100%, P=50%), the possible maximum radial temperature values fall within the range predicted by the two-regime model, highlighting the superiority of this model in fuel safety analysis.

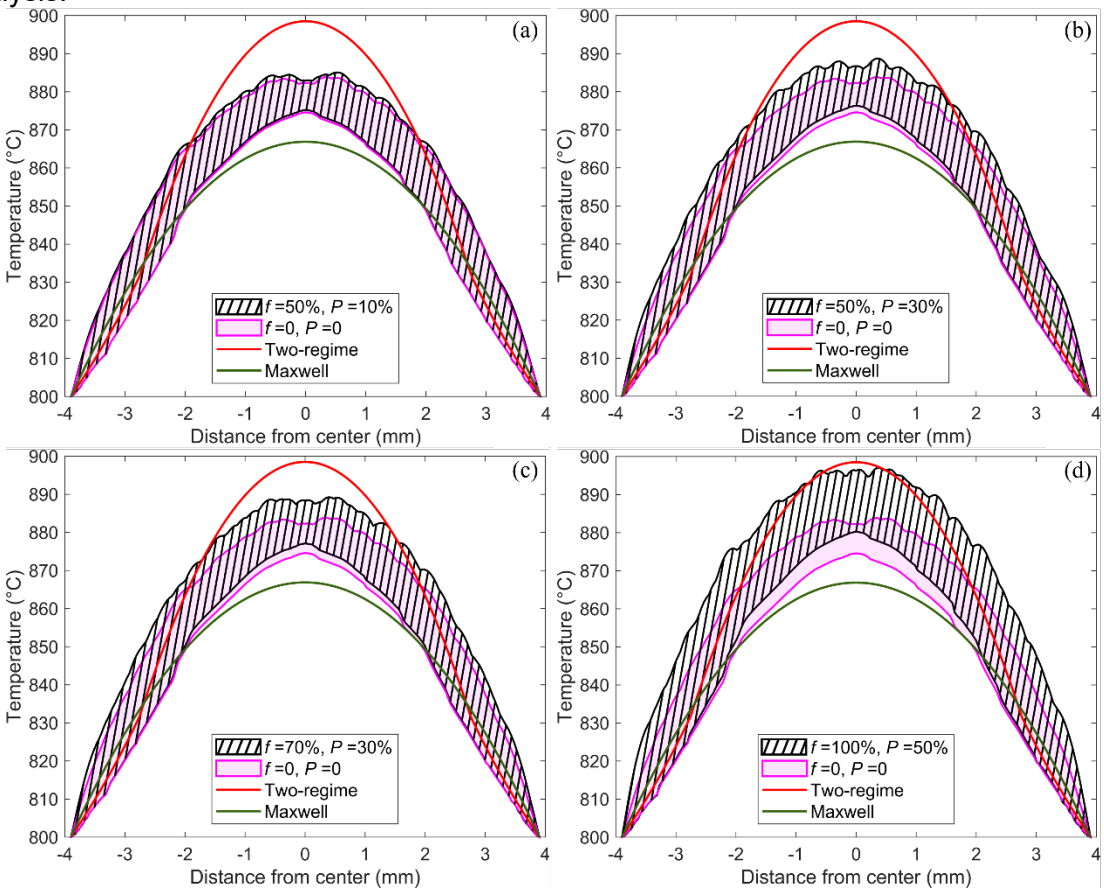

Fig. 7 Radial temperature distribution: (a) f=50%, P=10%; (b) f=50%, P=30%; (c) f=70%, P=30%; (d) f=100%, P=50%

4. Conclusion

In order to investigate the influence of additional thermal resistance caused by cracks in TRISO fuel particles with randomly distributed sizes and positions in a cylindrical matrix on the fuel temperature distribution, TRISO particles are generated within the cylindrical matrix using a relevant algorithm. Through numerical simulation, the three-dimensional temperature field distribution of the matrix is obtained, and sensitivity and uncertainty analyses are conducted on the effects of cracked particle proportion and the additional porosity caused by cracks on the fuel temperature distribution. The main conclusions of this study are as follows:

(1) The mean value of the maximum fuel temperature varies more significantly with changes in the additional porosity caused by cracks compared to the proportion of cracked particles. However, the magnitude of change with respect to both factors is small. Only under conditions where the additional porosity reaches 50% may an increase in peak temperature of over 0.9% (ΔT_{max} > 8 °C) occur, with a maximum increase of approximately 1.4% (ΔT_{max} = 12.2 °C).

(2) The standard deviation of the maximum fuel temperature is positively correlated with the additional porosity. While it initially increases, it then decreases with an increase in the proportion of cracked particles.

(3) The occurrence of cracks increases the dispersion of temperature distribution results for different scenarios at the same location, leading to a broader possible radial temperature distribution band. Compared to the proportion of cracked particles, the additional porosity

caused by cracks has a greater impact on the increase in fuel temperature levels.
(4) The study verifies that the two-regime model can conservatively predict the maximum temperature of TRISO-based FCM fuel, offering a safety margin. Even under extreme conditions, the simulated maximum fuel temperature is slightly lower than the prediction of this model. This model can be effectively applied in the design and safety analysis of TRISO-based FCM fuel. However, it is noteworthy that since the additional porosity caused by cracks is difficult to determine, this model still has limitations and further studies are needed.

References

[1] W.J. Kovacs, K. Bongartz, D. Goodin, "TRISO-coated HTGR Fuel Pressure-Vessel Performance Models", GA-A16807, General Atomics, October 1983.
[2] D.A. Petti, R. Hill, J. Gehin, H.D. Gougar, G. Strydom, F. Heidet, J. Kinsey, C. Grandy, A. Qualls, N. Brown, J. Powers, E. Hoffman, D. Croson, "Advanced Demonstration and Test Reactor Options Study", Idaho National Laboratory, INL/EXT-16-37867 Rev. 3, 2017.
[3] J. Wang, An Integrated Performance Model for High Temperature Gas Cooled Reactor Coated Particle Fuel, PhD Thesis, Massachusetts Institute of Technology, 2004.
[4] G.K. Miller, D.A. Petti, J.T. Maki, D.L. Knudson and W.F. Skerjanc, "PARFUME Theory and Model Basis Report," Idaho National Laboratory, INL/EXT-08-14497 Rev. 1, 2018.
[5] W.F. Skerjanc, J.T. Maki, B.P. Collin, D.A. Petti, "Evaluation of design parameters for TRISO-coated fuel particles to establish manufacturing critical limits using PARFUME", J. Nucl. Mater. 469 (2016) 99–105.
[6] T.A. Haynes, A. Battistini, A.J. Leide, D. Liu, L. Jones, D. Shepherd, M.R. Wenman, "Peridynamic modelling of cracking in TRISO particles for high temperature reactors", J. Nucl. Mater. 576 (2023) 154283.
[7] J.C. Maxwell, "A treatise on electricity and magnetism", Clarendon Press, 1873.
[8] Y.C. Chiew, E.D. Glandt, "The effect of structure on the conductivity of a dispersion", J. Colloid Interface Sci. 94 (1983) 90–104.
[9] D.a.G. Bruggeman, "Berechnung verschiedener physikalischer Konstanten von heterogenen Substanzen. I. Dielektrizitätskonstanten und Leitfähigkeiten der Mischkörper aus isotropen Substanzen", Ann. Phys. 416 (1935) 636–664.
[10] M. Liu, J. Thurgood, Y. Lee, D.V. Rao, "Development of a two-regime heat conduction model for TRISO-based nuclear fuels", J. Nucl. Mater. 519 (2019) 255–264.
[11] C. Wu, G. Yang, W. Zhang, X. Guo, M. Liu, "Numerical study of TRISO particles with random size and location distribution in cuboid and cylindrical matrix: A validation for two-regime heat conduction model", Nucl. Eng. Des. 423 (2024) 113193.
[12] G. Marsaglia, T.A. Bray, "A Convenient Method for Generating Normal Variables", SIAM Vol. 6, No. 3 (1964) 260–264.
[13] M. Liu, Y. Lee, D.V. Rao, "Development of effective thermal conductivity model for particle-type nuclear fuels randomly distributed in a matrix", J. Nucl. Mater. 508 (2018) 168–180.
[14] K.A. Terrani, L.L. Snead, J.C. Gehin, "Microencapsulated fuel technology for commercial light water and advanced reactor application", J. Nucl. Mater. 427 (2012) 209–224.